OCT 1 2 1993

ornl

ORNL/TM-12425

ORNL
MASTER COPY

OAK RIDGE
NATIONAL
LABORATORY

MARTIN MARIETTA

Analysis of Fission Product Release Data for German Fuel Sphere HFR-K3/3

R. C. Martin

No longer AT
David Hamm
3/3/2010

[redacted]

[redacted]

MANAGED BY
MARTIN MARIETTA ENERGY SYSTEMS, INC.
FOR THE UNITED STATES
DEPARTMENT OF ENERGY

This report has been reproduced directly from the best available copy.

Available to DOE and DOE contractors from the Office of Scientific and Technical Information, P.O. Box 62, Oak Ridge, TN 37831; prices available from (615) 576-8401, FTS 626-8401.

This report was prepared as an account of work sponsored by an agency of the United States Government. Neither the United States Government nor any agency thereof, nor any of their employees, makes any warranty, express or implied, or assumes any legal liability or responsibility for the accuracy, completeness, or usefulness of any information, apparatus, product, or process disclosed, or represents that its use would not infringe privately owned rights. Reference herein to any specific commercial product, process, or service by trade name, trademark, manufacturer, or otherwise, does not necessarily constitute or imply its endorsement, recommendation, or favoring by the United States Government or any agency thereof. The views and opinions of authors expressed herein do not necessarily state or reflect those of the United States Government or any agency thereof.

ORNL/TM-12425

Metals and Ceramics Division

ANALYSIS OF FISSION PRODUCT RELEASE DATA FOR GERMAN FUEL SPHERE HFR-K3/3

R. C. Martin

Date Published: September 1993

NOTICE

This document is an internal report of the New Production Reactors Program and contains PRELIMINARY AND TENTATIVE INFORMATION. It has not been given final patent clearance, and is for internal use only. If this document is to be given public release, it must be cleared through the site Technical Information Office which will see that proper patent and technical information reviews are completed in accordance with Energy Systems Policy.

[redacted]

Prepared for the
Office of New Production Reactors
U.S. Department of Energy
AF 20 50 10 0

Prepared by the
OAK RIDGE NATIONAL LABORATORY
Oak Ridge, TN 37831-6285
managed by
MARTIN MARIETTA ENERGY SYSTEMS, INC.
for the
U.S. DEPARTMENT OF ENERGY
under contract DE-AC05-84OR21400

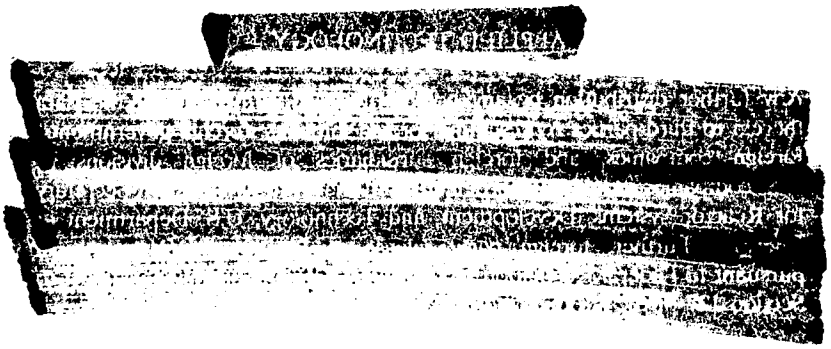

CONTENTS

Page

LIST OF FIGURES v
ABSTRACT 1
1. INTRODUCTION 1
2. SIGNIFICANCE OF VERFONDERN'S ANALYSIS 3
3. ANALYSIS OF HFR-K3/3 DATA USING THE GOODIN-NABIELEK MODEL 4
3.1 CESIUM-137 SPHERE RELEASE DATA 4
3.2 KRYPTON-85 SPHERE RELEASE DATA 5
3.3 IMGA DATA 7
4. ANALYSIS OF IMGA DATA USING THE MARTIN-GOODIN-NABIELEK MODEL 7
5. SIMPLE DIFFUSIVE ANALYSIS OF THE IMGA DATA 9
5.1 CHOICE OF COMPUTATIONAL DIFFUSION COEFFICIENTS 10
5.2 VARIATION IN SiC LAYER THICKNESS 11
6. CALCULATED CESIUM SPHERE RELEASE USING COMBINED MGN/DIFFUSION MODEL 11
7. RELATIONSHIP OF KRYPTON RELEASE TO CESIUM RELEASE 12
7.1 GN MODEL 12
7.2 OPyC FAILURE MODEL 12
8. DISCUSSION 15
8.1 SOURCE OF THE BIMODAL DISTRIBUTION 15
8.2 SHAPE OF THE BIMODAL DISTRIBUTION 15
8.3 SPECULATION ON FURTHER ANALYSIS AND MODELLING 16
9. CONCLUSIONS AND RECOMMENDATIONS 18
10. ACKNOWLEDGMENTS 20
11. REFERENCES 20
APPENDIX A: SHELL CODE DEVELOPMENT 23

LIST OF FIGURES

Figure		Page
1	Distribution of ^{137}Cs:^{144}Ce ratios normalized to Kernforschungsanlage preheating test values for German fuel spheres: (*a*) HFR-K3/3 and (*b*) HFR-K3/1. For comparison, a normal distribution based on the experimental data is plotted in the background[2]	2
2	Comparison of Goodin-Nabielek model predictions with experiment for HFR-K3/3 sphere release of cesium-137 and krypton-85	6
3	Reproduction of the Irradiated Microsphere Gamma Analyzer higher-inventory cesium-137 peak for sphere HFR-K3/3 using the Martin-Goodin-Nabielek model	9
4	Prediction of cesium-137 release from sphere HFR-K3/3 using the SHELL code	10
5	Reproduction of Irradiated Microsphere Gamma Analyzer bimodal cesium-137 inventory distribution using combined Martin-Goodin-Nabielek and diffusion models	13
6	Prediction of cesium-137 release from sphere HFR-K3/3 using combined Martin-Goodin-Nabielek and diffusion models. The predicted release was normalized to match the final experimental release	13
7	Prediction of krypton-85 release from sphere HFR-K3/3 using assumptions of the Goodin-Nabielek model and of 1% OPyC failure	14
8	Measured cesium-137 distributions in German particles and fuel spheres[15]	17
A.1	Comparison of fractional release predictions through OPyC layer using the analytical equation of H. Nabielek, using SHELL code, and using modified SHELL code. Diffusion coefficient of 10^{-14} m^2 s^{-1} was assumed	24
A.2	Comparison of fractional release predictions of krypton-85 through OPyC layer at 1800°C using the analytical equation of H. Nabielek, using SHELL code, and using modified SHELL code: (*a*) log scale and (*b*) linear scale	26

ANALYSIS OF FISSION PRODUCT RELEASE DATA FOR GERMAN FUEL SPHERE HFR-K3/3*

R. C. Martin

ABSTRACT

The fission product release data from the heating at 1800°C of German fuel sphere HFR-K3/3 and the Irradiated Microsphere Gamma Analyzer (IMGA) results for cesium inventory of the particles are analyzed. A recent analysis of the IMGA data[1] emphasizes the need for more than one fission product release mechanism in order to explain the data. The Goodin-Nabielek model for fission product release is applied to the sphere release data and IMGA data and found to be of limited validity. The Martin-Goodin-Nabielek (MGN) model provides a reasonable approximation of part of the IMGA distribution profile given appropriate model parameters. Incorporation of the assumption of particle failure during the thermal cycling process with the MGN model can reasonably approximate the bimodal cesium distribution represented by the IMGA data. Incorporation of an existing model for OPyC failure during irradiation provides a good approximation for the Kr-85 sphere release data. Other details of the experimental data and their relation to existing fuel performance models are discussed. Determination of the general validity of the models employed here requires further experimental and analytical evaluation.

1. INTRODUCTION

In report ORNL/M-2248,[1] K. Verfondern comments on the data for cesium-137 retention in particles from German fuel sphere HFR-K3/3 as measured by the Irradiated Microsphere Gamma Analyzer (IMGA) system at Oak Ridge National Laboratory (ORNL). This sphere underwent postirradiation heating at 1800°C for 100 h. The IMGA data for cesium retention indicate a bimodal inventory distribution [see Fig. 1(*a*)]. IMGA data for two other heated spheres (at 1600°C) show only a single Gaussian distribution for cesium inventory [e.g., see Fig. 1(*b*)]. No existing fuel performance model predicts a bimodal distribution for metallic fission product release from TRISO† particles such as that observed

*Research sponsored by the Office of New Production Reactors, U.S. Department of Energy, under contract DE-AC05-84OR21400 with Martin Marietta Energy Systems, Inc.

†Tristructural (buffer, SiC, PyC) isotropic coating design.

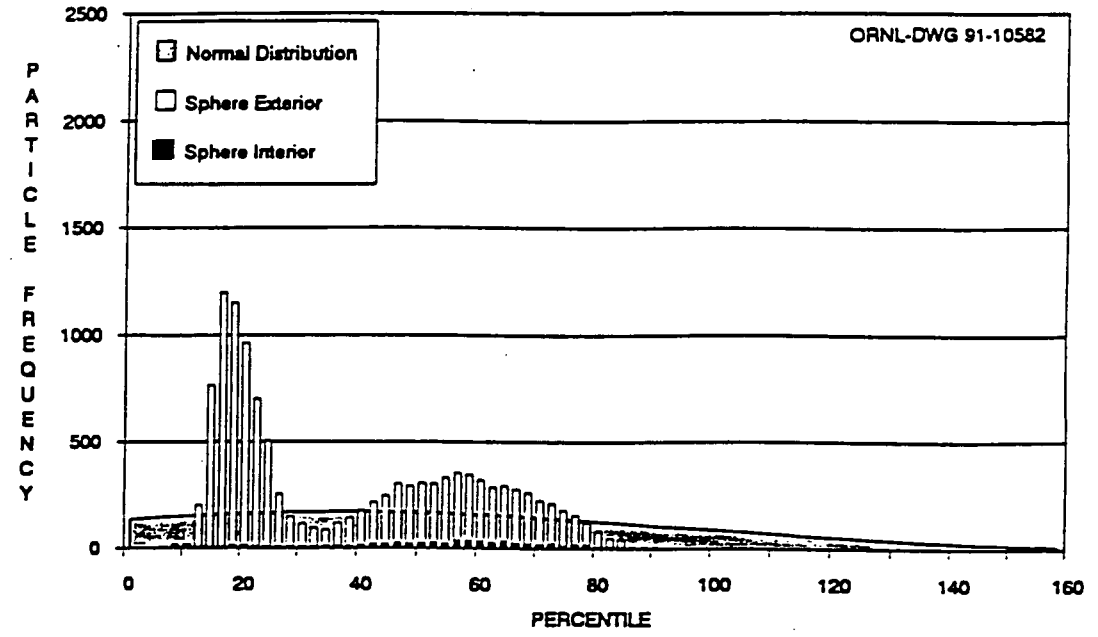

(a)

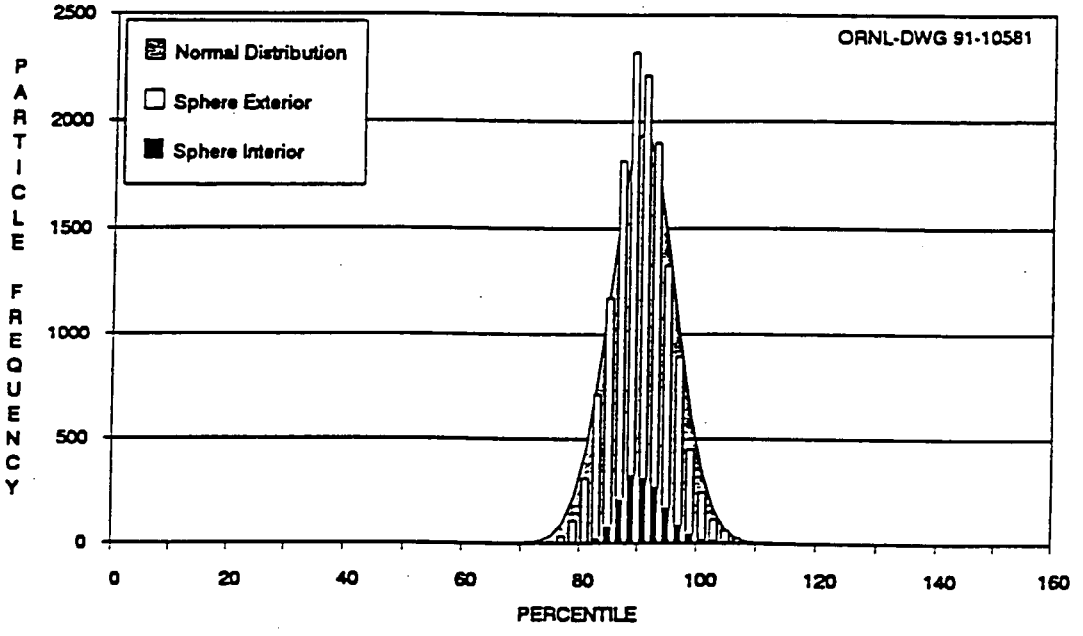

(b)

Fig. 1. Distribution of ^{137}Cs:^{144}Ce ratios normalized to Kernforschungsanlage preheating test values for German fuel spheres: (*a*) HFR-K3/3 and (*b*) HFR-K3/1. For comparison, a normal distribution based on the experimental data is plotted in the background.[2]

in Fig. 1(*a*). As such, analysis and explanation of these results could provide improved understanding of the mechanisms of cesium (and other fission product) release from TRISO particles. A potentially significant factor in this heating experiment was the sudden shutdown and cooling of the furnace at 25.5 h into the 100-h test.

The IMGA particle inventory data can also be compared with the data for total cesium release from the HFR-K3/3 sphere obtained during the German furnace test. These data are not quantitatively comparable, as a significant fraction of cesium is retained in the matrix graphite of the sphere, and, in the case of sphere HFR-K3/3, even if this is taken into account, the aggregate particle inventory still does not correlate well with the sphere release data due to a possible accumulation of experimental errors. Lack of a mass balance between sphere release and IMGA results permits only qualitative comparisons between IMGA and sphere release data. The sphere release data for krypton-85 can also be used to provide additional information on particle performance.

2. SIGNIFICANCE OF VERFONDERN'S ANALYSIS

Much of Verfondern's analysis applies the German FRESCO-II diffusion code[3] to approximation of the data for cesium-137 release from the HFR-K3/3 sphere during heating. Details of the numerical results are available in this reference and will not be emphasized here. Verfondern combines the diffusion model of FRESCO-II with an assumed particle failure profile based on the IMGA observations to obtain both a bimodal distribution of cesium release from the particles and a prediction of overall sphere release comparable to that observed with the furnace test data. Although the models employed are capable of approximating the total sphere release, the bimodal distribution is only approximated in a form similar to two delta functions rather than the broader distributions evident in Fig. 1(*a*).

The most important points of Verfondern's analysis and the implications for existing fuel performance models are the following:

1. The higher-inventory (lower-release) component of Fig. 1(*a*) is attributed to a diffusive release mechanism that can be defined by a single diffusion coefficient.
2. The lower-inventory component of Fig. 1(*a*) is attributed to release from particles that functionally failed due to thermal stress induced by the rapid furnace cooldown at 25.5 h into the heating test. This assumption is supported by the observation that fewer particles in the interior of the sphere were represented in the lower-inventory component than those in the exterior region of the sphere. The interior of the sphere would be expected to cool less rapidly, resulting in lower thermal stresses on the interior particles.
3. Although the lower-inventory component averaged 80% cesium-137 release, the exposed kernel release model used in FRESCO-II would predict virtually 100% release from any failed particle under the heating conditions of the test. Even the higher-inventory component averages a significant 40% release, which would also fall under the category of functionally failed particles. The common assumption of complete loss of retention of cesium once the SiC layer fails at high temperatures is thus not supported by the IMGA data for sphere HFR-K3/3. A related assumption that particles with failed SiC layers act like exposed kernels with respect to cesium release is also not supported.

Although FRESCO-II is formulated to consider diffusion through intact coating layers, as well as particle failure, these calculations are unique in defining the failure function not in terms of observed krypton-85 release during heating but in assuming some significant magnitude of failure upon rapid sphere cooldown. Limitations in Verfondern's analysis center on two points:

1. The calculated bimodal distribution is represented by two sharp delta-function-like inventory distributions rather than the broader peaks indicated by the IMGA data.
2. Although the value of the diffusion coefficient for cesium in SiC, which is used in the analysis, is bracketed by previously published values, its choice appears arbitrary.

3. ANALYSIS OF HFR-K3/3 DATA USING THE GOODIN-NABIELEK MODEL

Verfondern's consideration of diffusive cesium transport through SiC contrasts with the Goodin-Nabielek (GN) SiC failure model which states that "retention of Cs by the fuel kernel or by pyrocarbon is negligible at the point in time when SiC failure begins to occur."[4] Such a hypothesis implies 100% cesium release at the point of SiC failure, which is in obvious contradiction to the IMGA data of Fig. 1(*a*). The basic assumptions of the GN model are that:

1. Cesium release is used as the indicator of particle failure.
2. Cesium does not diffuse through intact SiC.
3. At temperatures at and above 1600°C, the fractional release of cesium from a particle is represented by a step function from 0 to 1 at the instant of SiC failure.
4. After SiC failure, the subsequent release of krypton from the particle is governed by diffusion through the OPyC layer.

After the cesium escapes from the particle, some fraction is retained by the matrix graphite of the sphere. The 1989 version of the GN model[5] uses a correction factor to convert sphere release to particle release. Because of the ambiguity inherent in this "matrix release fraction" as stated, the following analyses will consider only the experimental data for total sphere release rather than attempting to extrapolate the sphere release data to the particle release.

3.1 CESIUM-137 SPHERE RELEASE DATA

The 1989 revision of the GN model is defined by the following equations:

$$\Phi(t) = 1 - 2^{-(kt)^m} , \qquad (1)$$

and

$$k = 5.029 \times 10^{-4}\ e^{-65{,}540/T}\ \max\ (f_{SiC}^{2.09} \cdot \Gamma^{0.041} \cdot T_{irr}^{4.14},\ 2.74 \times 10^{14}) \quad , \qquad (2)$$

where

$\Phi(t)$ = SiC failure fraction (= fractional cesium release from the particles),
k = failure frequency factor (h^{-1}),
t = heating time (h),
m = Weibull parameter,
T = heating temperature (K),
f_{SiC} = fission density (10^{26} fissions m^{-3} inside the SiC layer),
Γ = fast neutron fluence (10^{25} neutrons m^{-2}, E > 0.1 MeV),
T_{irr} = irradiation temperature (K).

The value $m = 2$ is used for heating tests.[5] The term *max* in Eq. (2) specifies the use of the maximum of the two terms which follow. Using the values appropriate for sphere HFR-K3/3:

T = 1800°C,
f_{SiC} = 6.7,
Γ = 6.0,
T_{irr} = 1273,

the following equation is obtained for the cesium release from the sphere as a function of time:

$$\Phi(t) = 1 - 2^{-(0.00383\,t)^2} \quad . \qquad (3)$$

The fractional cesium release predicted by Eq. (3) is compared with the experimental sphere release[6] in Fig. 2. The agreement is good except for the initial 25 h of heating.

3.2 KRYPTON-85 SPHERE RELEASE DATA

Although Goodin does not show predictions of krypton release,[5] the assumptions of the model can be applied with the reference diffusion coefficient of krypton in pyrocarbon and with the cesium release data to predict the krypton-85 sphere release. The diffusion coefficient for krypton in pyrocarbon is given by Goodin as:[5]

$$D\ (m^2 s^{-1}) = 2.90 \times 10^{-8}\ e^{-35{,}000/T} + 2.02 \times 10^{5}\ e^{-111{,}000/T} \quad , \qquad (4)$$

where

T = heating temperature (K).

ORNL-DWG 93-12803

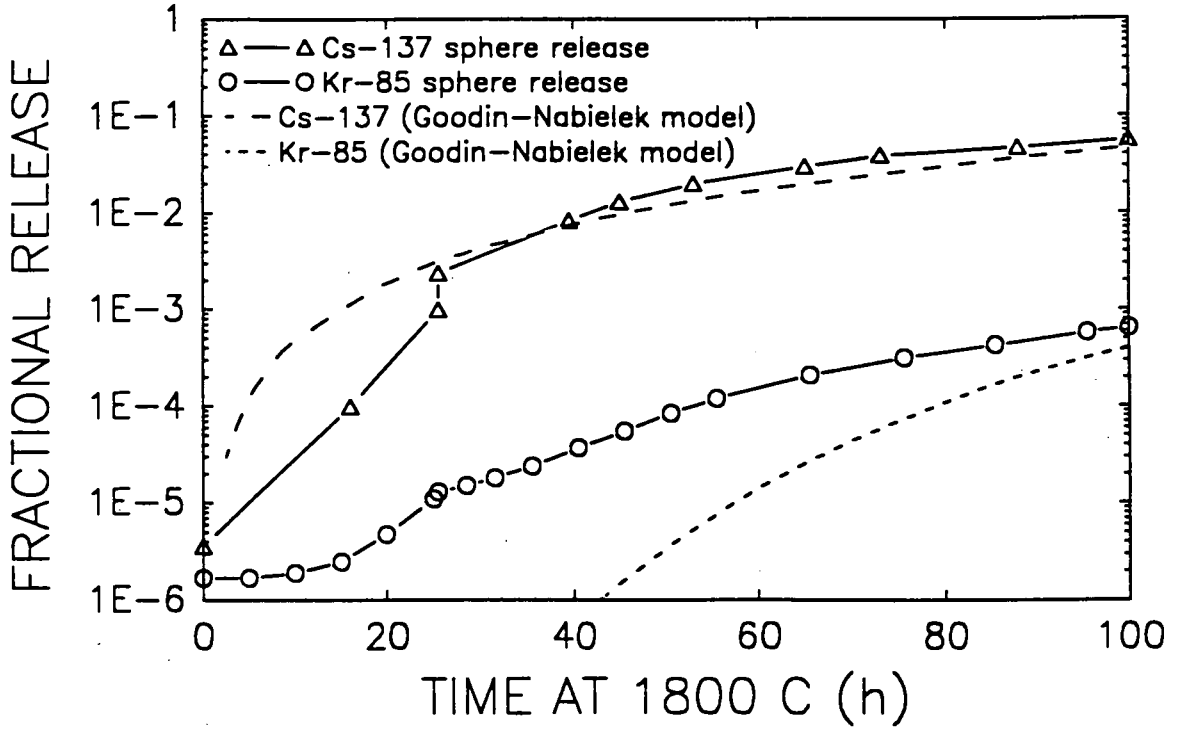

Fig. 2. Comparison of Goodin-Nabielek model predictions with experiment for HFR-K3/3 sphere release of cesium-137 and krypton-85.

The cesium-137 fractional sphere release data can be approximated by the following polynomial expression:

$$\log(FR_{Cs}) = 5.96\times10^{-6}\,t^3 - 1.55\times10^{-3}\,t^2 + 0.138\,t - 5.52 \quad , \qquad (5)$$

where

t = heating time (h).

Equation (5) can be used to calculate the incremental SiC failure as a function of time, and the SHELL code for diffusion through a single layer (ref. 7 and Appendix A) can be used in conjunction with Eq. (4) to predict the time-dependent fractional krypton release resulting from each increment of SiC failure. The calculated krypton-85 release is shown in Fig. 2; agreement with the experimental data is found to be wanting except toward the end of the heating test. Consideration of cesium retention by the matrix graphite would increase the end-of-test krypton release by a factor of two, which agrees well with the experimental release but does not significantly reduce the discrepancy at the shorter heating times.

3.3 IMGA DATA

Although the predicted cesium sphere release is generally satisfactory, the validity of the assumptions of the GN model related to krypton release is not confirmed by this analysis. This model is particularly weak in comparison with the IMGA data of Fig. 1(*a*). The model assumptions predict two delta-function-like distributions for particle cesium inventory: retention should be 100% if the SiC layer is intact and 0% if it is not. No provision for a distribution of inventory values such as observed in Fig. 1(*a*) is possible using the existing assumptions of the model. Although modification of model assumptions might provide such a distribution, a complete rederivation of the model would likely be required. The model as it exists is not readily amenable to reproducing the IMGA data.

4. ANALYSIS OF IMGA DATA USING THE MARTIN-GOODIN-NABIELEK MODEL

The Martin-Goodin-Nabielek (MGN) model[8] was developed in an attempt to improve the GN model. The MGN model uses the failure formalism of the GN model, Eq. (1), but considers failure to initiate diffusion of cesium through SiC rather than instantaneously releasing the cesium from the particle. As stated by J. L. Martin et al., the model "describes particle failure by a mechanism beginning with SiC grain boundary damage caused by SiC thermal decomposition, leading to permeability of the SiC layer ... after which the Cs is released through the SiC by a diffusive process, most likely a surface diffusion process as proposed by [D. T.] Goodin ..."

Although the MGN model does not deny the possibility of cesium diffusing through intact SiC, it considers such diffusion to be insignificant relative to diffusion through damaged SiC and thus disregards any contribution to cesium release by intact SiC. The MGN model has not been extended to consider krypton release.

J. L. Martin et al. recommend the following values for use in Eq. (1):[8]

k = 0.00448 h^{-1} at 1800°C,
m = 2.0.

After 100 h, use of these values predicts an SiC failure fraction of 13%. This prediction of 87% intact particles is obviously inconsistent with the IMGA data of Fig. 1(*a*). If the MGN model is valid, then other model parameter values must be used. However, it should be noted that the MGN model parameters given by J. L. Martin et al. were chosen to provide agreement with the sphere release data rather than the IMGA data, and modelling of these two data sets could not use the same model parameters for the reasons given previously (lack of cesium mass balance between the two data sets, etc.).

J. L. Martin et al. recommended the use of the following diffusion coefficient for cesium in failed SiC at 1800°C:

$$D_{MGN} = 1.73 \times 10^{-13}\ m^2 s^{-1} \quad , \tag{6}$$

which is ten times larger than a reference diffusion coefficient derived by Myers.[9] Rather than using a convenient diffusion coefficient which provides agreement between model and experiment, a more self-consistent modelling approach is to use independently derived

diffusion coefficients and adapt the model to the existing published data. The published diffusion coefficients used in the following analysis were derived by Myers[9] for cesium diffusion in two different SiC structures (characterized by laminar or columnar features). These two diffusion coefficients were applied to the MGN model, with the diffusion coefficient assumed to change from the laminar to the columnar value at the point of SiC failure as defined by the Weibull distribution. The columnar diffusion coefficient is approximately a factor of ten greater than the laminar at 1800°C; thus, the assumptions of the MGN model are not violated by the use of a nonzero diffusion coefficient prior to SiC failure. At 1800°C, the laminar and columnar diffusion coefficients are calculated to be:

$$D_{lam} = 1.24 \times 10^{-15}\ m^2 s^{-1} \quad , \tag{7}$$

and

$$D_{col} = 1.75 \times 10^{-14}\ m^2 s^{-1} \quad . \tag{8}$$

To derive the Weibull parameters from the cesium sphere release data, it is noted that the maximum rate of change in cesium release occurs at approximately 55 h into the heating test, as determined using Eq. (5). The assumption is made that the SiC failure fraction is 0.5 at this time. Given a value for m, a value for k can then be derived for use in Eq. (1). If we choose $m = 2$ as suggested by Goodin[5] and J. L. Martin et al.,[8] the following Weibull distribution is derived:

$$\Phi(t) = 1 - 2^{-(0.0182\,t)^2} \quad , \tag{9}$$

or using $m = 5$ for comparison (as commonly used in pressure-vessel models), the following is obtained:

$$\Phi(t) = 1 - 2^{-(0.0182\,t)^5} \quad . \tag{10}$$

These values for k vary by a factor of four to five from those recommended by Goodin (0.00383) and J. L. Martin et al. (0.00448).

The time-dependent SiC failure fraction defined by Eqs. (9) or (10) can be combined with calculations using the SHELL diffusion code (see Appendix A) to simulate transition of the diffusion coefficient to the larger value at the time of failure. The resulting distributions are shown in Fig. 3 for several assumed values of the Weibull parameter. Although the range of one of the bimodal peaks of Fig. 1(a) is approximated using $m = 2$, the shape of the peak is not. The calculated curve is skewed toward greater fractional release, and the unfailed fraction of particles after 100 h generates the anomalous peak at 94% fractional inventory. The value $m = 5$ better approximates the experimental distribution, but best agreement is obtained for $m = 4$, as shown in Fig. 3.

By deriving the parameter k from the sphere release data, choosing a judicious value of m, and applying a previously published range of diffusion coefficients for Cs in SiC, the low-release component of the bimodal IMGA distribution is well approximated by the MGN model. However, the MGN model as presented would not predict the second, high-loss peak unless a second failure mechanism function was added with its own failure function and unique k and m values. The results of this MGN model cannot be compared to the sphere release data without consideration of this second peak.

ORNL-DWG 93-12804

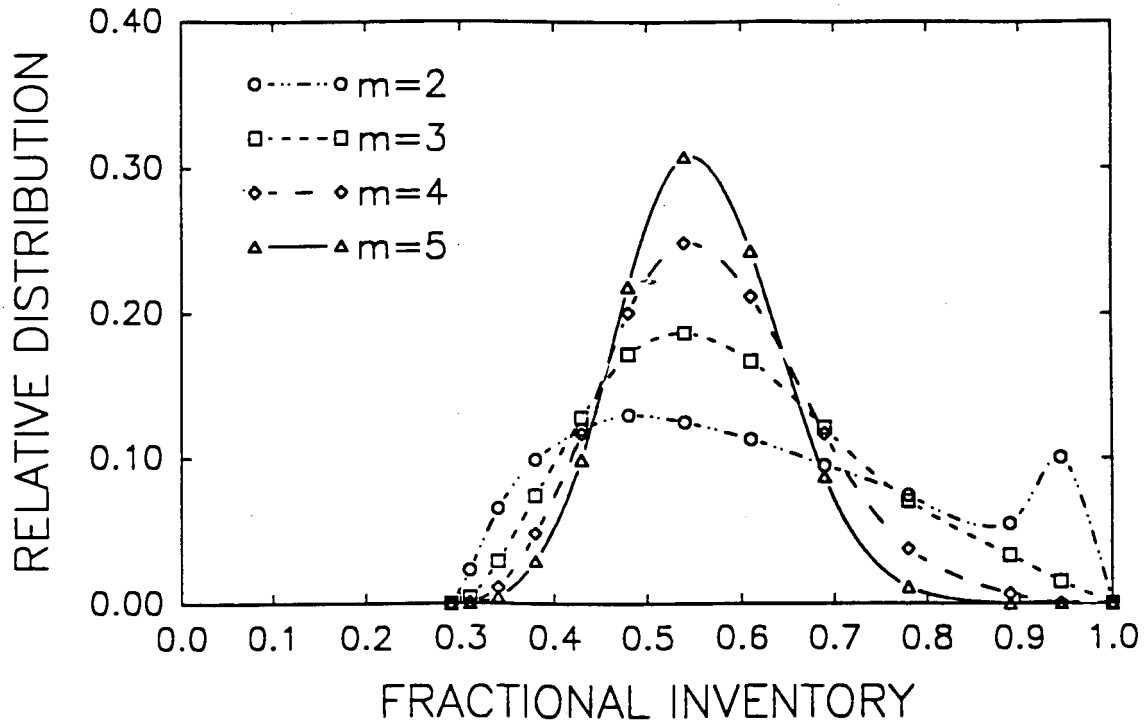

Fig. 3. Reproduction of the Irradiated Microsphere Gamma Analyzer higher-inventory cesium-137 peak for sphere HFR-K3/3 using the Martin-Goodin-Nabielek model.

5. SIMPLE DIFFUSIVE ANALYSIS OF THE IMGA DATA

An analysis was performed to determine whether modelling of fission product release based on diffusion only could approximate some or all of the bimodal cesium inventory distribution. These calculations were based on the SHELL code, a simple analytical approach to calculating the diffusive release through a thin spherical shell.[7] More information on this code is provided in Appendix A. Use of the laminar diffusion coefficient of Eq. (7) in a SHELL calculation accurately reproduces the measured sphere cesium release (see Fig. 4) but does not consider the cesium retained in the graphite. Consideration of this retention would require use of a computational diffusion coefficient approximately 50% larger than that of Eq. (7). Due to the mass balance considerations discussed in §1, reproduction of the IMGA data for particle inventories would require still larger diffusion coefficients.

ORNL-DWG 93-12805

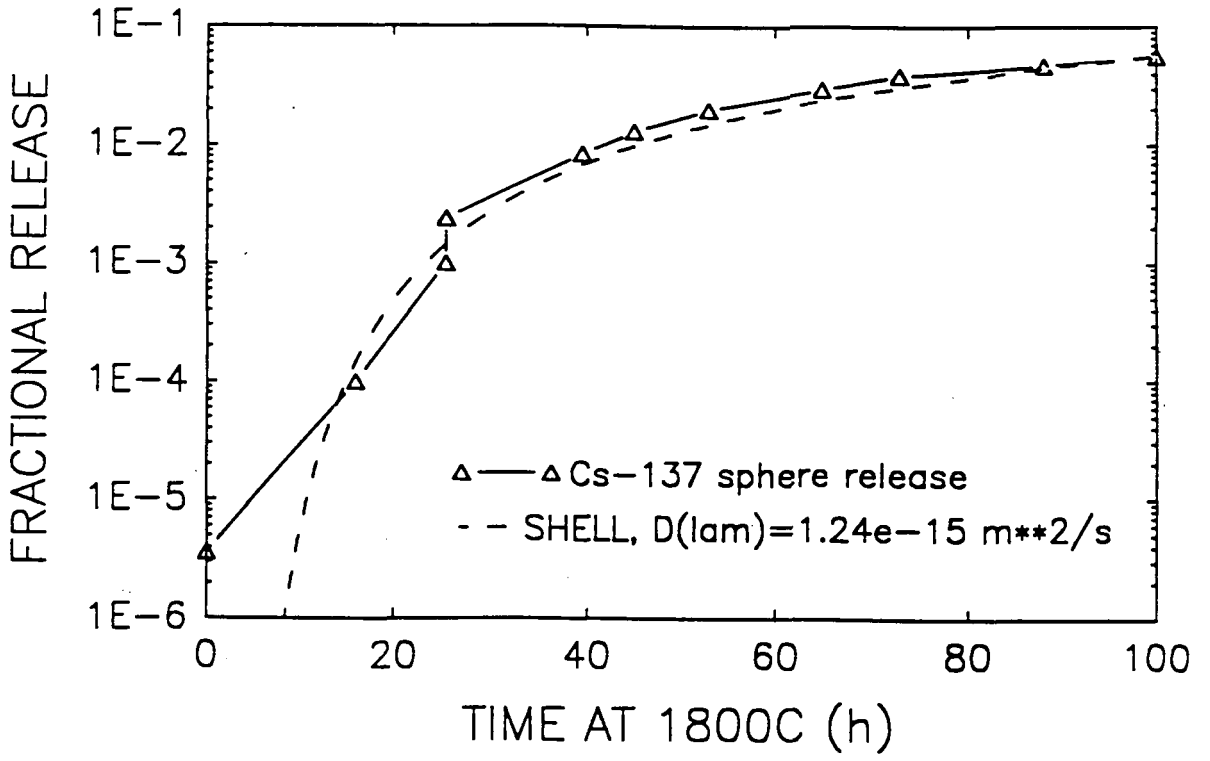

Fig. 4. Prediction of cesium-137 release from sphere HFR-K3/3 using the SHELL code.

5.1 CHOICE OF COMPUTATIONAL DIFFUSION COEFFICIENTS

For comparative purposes, the value for D_{lam} in Eq. (7) was used to predict the cesium inventory of the particles after 100 h of heating at 1800°C. SHELL calculations indicate the average inventory would be expected to be about 95%, which is too large compared to the IMGA data. The two peaks of the bimodal distribution [see Fig. 1(*a*)] indicate average cesium inventories of approximately 57 and 19%. Calculations using D_{col} over 100 h indicate a 29% average inventory, intermediate between the bimodal peaks.

To reproduce the low-inventory peak of Fig. 1(*a*), one can combine the MGN model assumption of a transition to a larger diffusion coefficient at the point of SiC failure and Verfondern's assumption of SiC failure at 25.5 h into the heating cycle due to thermal cycling effects. Using the values of D_{lam} for unfailed SiC and D_{col} for failed SiC after 25.5 h, one would predict average cesium inventories of 38%, representing the average of the bimodal peaks and close to the average particle loss of approximately 40%. If, instead of D_{col}, one uses a diffusion coefficient of 3.1×10^{-14} m^2 s^{-1}, SHELL can approximate the average inventory of the low-inventory peak. This value of the computational diffusion coefficient will be referred to as D_{fail}. D_{fail} is nearly twice the value of D_{col}.

The higher-inventory peak is too broad to reproduce using a diffusive analysis based on a single diffusion coefficient. The analysis using the MGN model adequately reproduced this peak; therefore, this simple diffusive analysis will only be applied to the low-inventory peak.

5.2 VARIATION IN SiC LAYER THICKNESS

Diffusion calculations seldom consider the variation in SiC thickness inherent in the manufacturing process as a significant factor in fission product release. For low levels of release, this variation will not be significant, but as release approaches 100%, the variation in thickness will result in significant variations in diffusive fractional release. The standard deviation in SiC layer thickness of the HFR-K3/3 particles is reported to be 1.8 μm for an average thickness of 36 μm (ref. 10). For SiC thicknesses of 34.2 to 37.8 μm, the average inventory after 100 h of heating was calculated assuming a transition from D_{lam} to D_{fail} at 25.5 h, with the average inventory ranging from 17 to 20%. Although this inventory distribution is narrower than that apparent in Fig. 1(*a*), it is more realistic than the delta-function distributions predicted by the FRESCO-based calculations of Verfondern.[1]

Variations in SiC layer thickness could be more significant for the U.S. program, with an allowable coating thickness variation from 30 to 40 μm (ref. 11). For SiC thicknesses of 30 to 40 μm, reproduction of the previous calculations indicates fractional inventories would vary from 13 to 22%.

One could postulate some time dependence in the transition of D_{lam} to D_{fail} to broaden the calculated low-inventory peak, and one could postulate a less abrupt transition from D_{lam} to D_{col} in §4. However, we are more interested here in the qualitative features of the model-to-data relationship and its relevance to the other heating tests. For this reason, we truncate this detailed analysis of the IMGA data at this point, combine those features of §4 and §5 which can approximate the IMGA distribution, and extend the analysis to the overall sphere release data of Schenk et al.[6]

6. CALCULATED CESIUM SPHERE RELEASE USING COMBINED MGN/DIFFUSION MODEL

If we accept an SiC failure mechanism that results from the effects of thermal cycling during furnace shutdown (or some other less obvious mechanism but which produces comparable results), we could postulate SiC layer failure by cracking, resulting in rapid but noninstantaneous cesium release which might be modelled using a large diffusion coefficient for cesium in SiC (e.g., D_{fail}). However, such a failure mechanism is not representative of existing models which predict gradual particle-to-particle SiC failure at high temperature.* For example, cesium release from thermally decomposing or corroding SiC would likely be characterized by a time-dependent increase of the diffusion coefficient with values less than any typical for a structurally cracked SiC layer. The gradual formation of interconnected porosity should not suddenly release a burst of cesium if the pores are small.

---

*It should be noted that this experiment is unique in the rapid cooldown of the fuel. Although existing models cannot explain the IMGA results for sphere HFR-K3/3, a conclusion that the models are thus invalid for typical reactor conditions or standard heatup tests does not necessarily follow. Observation of bimodal distributions in other heating tests would address this issue directly.

Using this rationale, it may be reasonable to combine the particle inventory distribution obtained using the MGN model with that obtained from the diffusion calculation for the low-inventory component of the distribution, resulting in an overall inventory distribution that qualitatively looks something like Fig. 5. The peak heights were arbitrarily adjusted to approximate the relative peak heights in Fig. 1(*a*). The IMGA data indicate approximately 58% of the particles occupy the higher-inventory component of the distribution while 42% occupy the low-inventory component. The low-inventory component, as predicted for the U.S. particle design (larger variation in SiC thickness) but using the same diffusion parameters, is also shown in Fig. 5 for comparison.

Assuming these inventory distributions apply to the model represented by Fig. 5, one can predict the overall cesium sphere release based on this combined MGN/diffusion model. However, any sphere release predictions based on the IMGA data must be normalized to the experimental data due to the lack of mass balance between the two experimental approaches. The result is shown in Fig. 6, with the predicted release normalized to match the experimental sphere release at the end of heating. This normalized prediction compares reasonably with the experimental data over all but the initial 35 h of the heating test. This calculation does not consider the cesium retained within the matrix graphite, although this should not be significant for the normalized calculations. Predictions of fractional cesium release below 10^{-5} are not significant because of the presence of heavy metal contamination within the fuel sphere.

7. RELATIONSHIP OF KRYPTON RELEASE TO CESIUM RELEASE

7.1 GN MODEL

The basic assumption of the GN model is that cesium release indicates failure of the SiC layer, and krypton release would parallel the cesium release were it not for retention by the OPyC layer. Thus, given the experimental cesium release, one should be able to approximate the krypton release using a diffusion calculation, except for the error introduced by retention of cesium by the matrix graphite of the sphere (a factor of about two at the end of heating for sphere HFR-K3/3). Krypton retention by the matrix graphite is insignificant and thus introduces no error, as is the case for cesium. These results were shown in Fig. 2. Agreement between the experimental data and the calculated krypton release is not good except toward the end of the heating test, indicating some problem with the GN model assumptions for this heating test.

7.2 OPyC FAILURE MODEL

The modular high-temperature gas-cooled reactor (MHTGR) program in the United States uses a fuel performance model for irradiation-induced failure of the OPyC layer from fast neutron fluence effects. For example, a typical value for OPyC failure is considered to be 3% (ref. 12) although this value varies from experiment to experiment. The German program does not employ a comparable model for irradiation-induced OPyC failure.[13] The

ORNL-DWG 93-12806

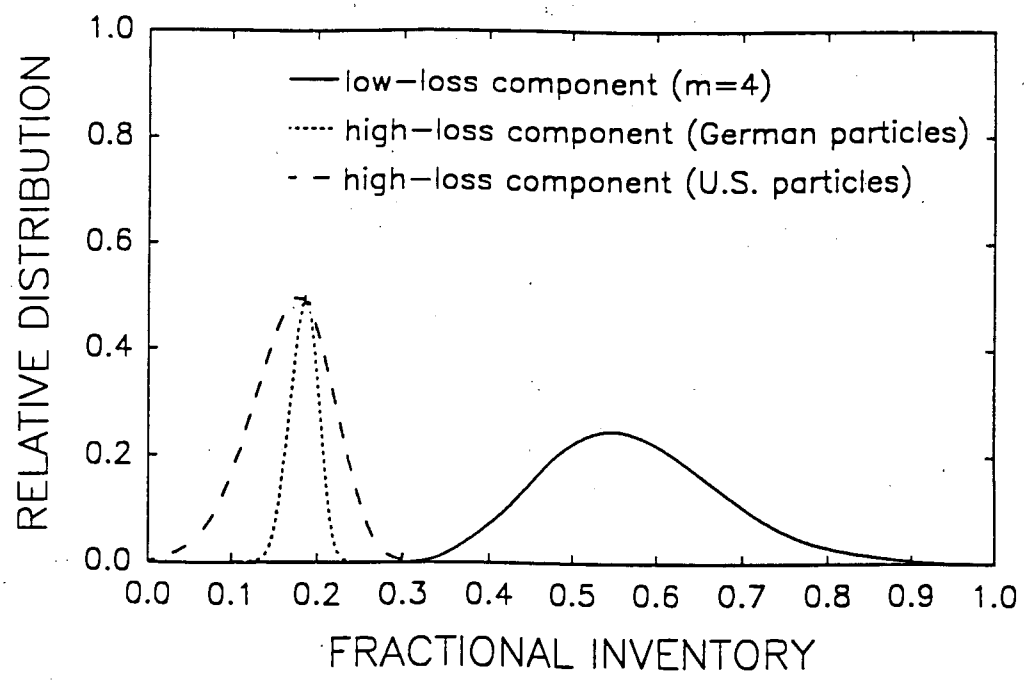

Fig. 5. Reproduction of Irradiated Microsphere Gamma Analyzer bimodal cesium-137 inventory distribution using combined Martin-Goodin-Nabielek and diffusion models (relative peak heights are arbitrary).

ORNL-DWG 93-12807

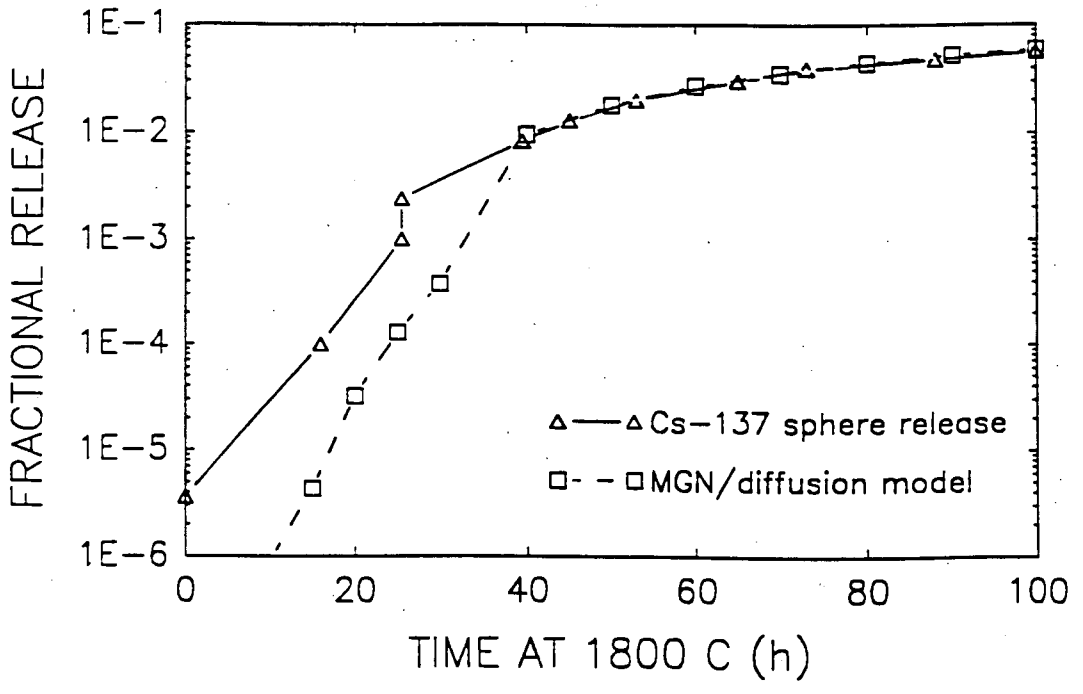

Fig. 6. Prediction of cesium-137 release from sphere HFR-K3/3 using combined Martin-Goodin-Nabielek and diffusion models. The predicted release was normalized to match the final experimental release.

assumptions of the GN model would suggest that cesium and krypton release from a particle with a failed OPyC layer should be similar, and such a contribution to total krypton release could be significant.*

As a test of this OPyC failure model, let us assume an OPyC failure rate of 1% for the particles of sphere HFR-K3/3. The contribution to total krypton release from this failure mechanism would then total 1% of the measured cesium release, and the normalized time-dependent krypton release profile should approximate that of cesium. To visualize this relationship, the cesium sphere release data are reduced to 1% of their experimental value and plotted in Fig. 7. The agreement with the experimental krypton-85 sphere release is obviously much better than that of the GN model.

If one assumes that both the GN approach and 1% OPyC failure are valid, then both these contributions to krypton release should be combined for the total sphere release. This result is also plotted in Fig. 7, and the agreement with the experimental data is again

ORNL-DWG 93-12808

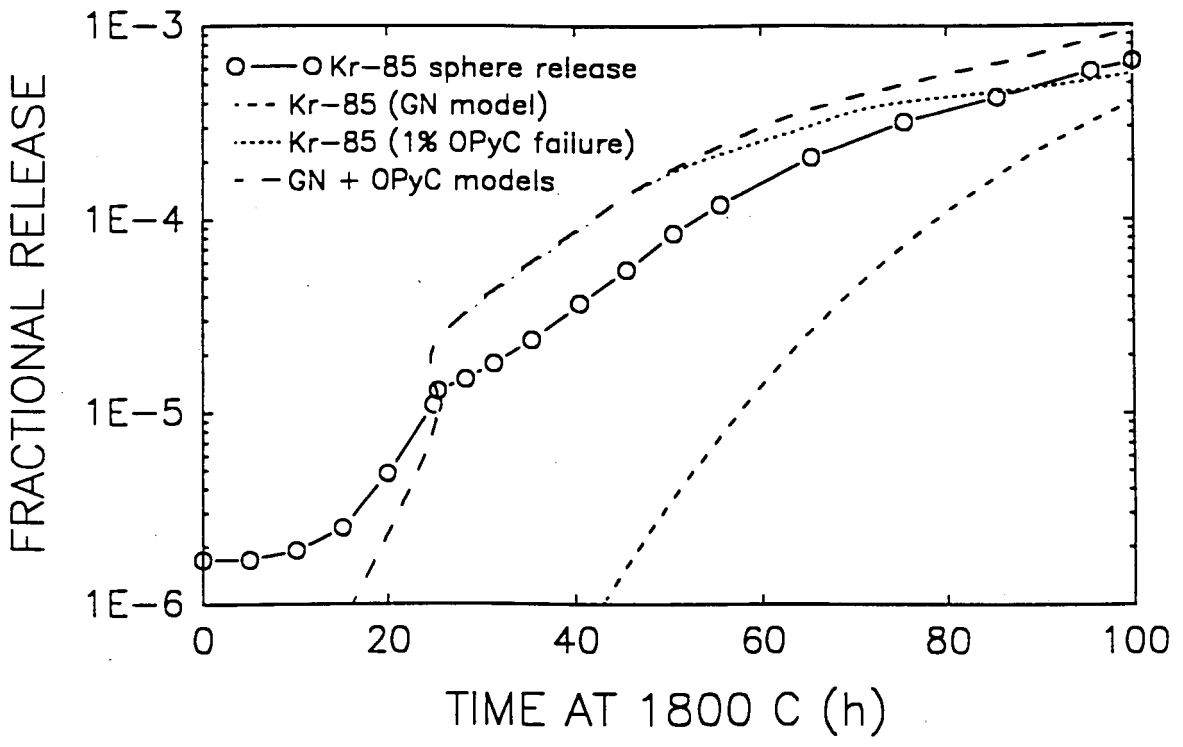

Fig. 7. Prediction of krypton-85 release from sphere HFR-K3/3 using assumptions of the Goodin-Nabielek model and of 1% OPyC failure.

*Experimental results from irradiation capsule HRB-16 suggest a more complicated relationship, with some influence of IPyC and/or buffer layers on krypton release.[14]

reasonable. Although the GN model in itself may not accurately predict the time-dependent krypton release, this model may not be inconsistent with the experimental data if combined with a model for irradiation-induced failure of the OPyC layer.

8. DISCUSSION

8.1 SOURCE OF THE BIMODAL DISTRIBUTION

One can only speculate on the physical mechanisms that produce the bimodal inventory distribution without detailed inspection of the particles themselves or other supporting evidence. The fact that the particles which release the most cesium are predominantly located toward the exterior of the sphere may provide some evidence. Reduction of the neutron flux at the center of the sphere by self-shielding is believed to be only about 10%, so differential neutron irradiation damage would not be expected to cause such distinct differences in inner versus outer particle behavior.

A more likely cause is the differential thermal environment of the fuel particles. The temperature profile across the sphere during irradiation is symmetric about the center; thus, the temperature gradient is greater toward the outside of the sphere. Temperature gradients are known to enhance both kernel migration and fission product corrosion of the SiC layer (although the former is not as great a concern for the German fuel design). A potential thermal failure mechanism is the rapid cooling of the sphere during unplanned furnace shutdowns, such as occurred during the HFR-K3/3 test. The exterior of the sphere cools faster than the center; thus, thermal stresses on the outer particles would be greater. Whether these stresses are significant enough to cause particle failure is a matter of debate, although there is some evidence that other German spheres, which were similarly reheated, tended to exhibit greater fission product release than spheres heated only once. Some synergism between thermal cycling effects and thermal-gradient-induced degradation of the SiC is not inconceivable. Any proposed mechanism for the observed release patterns is only speculation without additional information or analysis.*

Although the other two German spheres examined with IMGA did not exhibit such a bimodal distribution, these spheres were not heated above 1600°C and thus were not subjected to the strenuous thermal conditions of the HFR-K3/3 test. As such, those results may not be directly comparable.

8.2 SHAPE OF THE BIMODAL DISTRIBUTION

A distinctive feature of the bimodal distribution is the greater width of the higher-inventory peak than that of the low-inventory peak. On first analysis, one might expect the

---

*R. N. Morris suggests an alternative hypothesis. While at temperature, fission products diffuse into the SiC and locally change the phase structure of the SiC. When the temperature suddenly drops, a new phase could form or differential thermal expansion of the neighboring phases could induce cracking within the SiC. This hypothesis is consistent with observations of fission-product-induced corrosion of SiC.

distribution to broaden as the loss increases. An alternative explanation might be that the failure mechanism involved in intermediate releases exhibits more particle-to-particle variability (e.g., developing and interconnecting porosity), while the low-inventory peak is typical of distinct SiC failure (e.g., a microcrack in the SiC layer). As such, we might consider the low-inventory peak to be representative of a completely failed SiC layer and the release from these particles to be representative of release from completely failed particles.

It is significant that these low-inventory particles, although obviously failed with respect to retention capabilities, continue to retain nearly 20% of their total inventory. Existing failure models and models for cesium release from exposed kernels would not predict this much retention after prolonged heating at 1800°C.

If one considers possible mechanisms which could account for a nearly constant 20% retention of cesium in failed particles, the sorption of cesium by the carbonaceous layers of the particle seems feasible. Figure 8 (ref. 15) indicates the fractional distribution of cesium-137 across a particle for several fuel spheres. The particle from sphere HFR-K3/3 retained over 50% of its cesium-137 inventory within the buffer layer at the end of the heating test (this particle apparently represents the higher-inventory component of the bimodal distribution). This retention fraction is also comparable to that for sphere HFR-K3/1 (heated at 1600°C for 500 h). Figure 8 suggests that sorption of cesium is more significant within the buffer layer than within the kernel for retention at high temperatures. Possible effects of the buffer layer on fission product release are not considered in current fuel performance models. These data suggest that equilibrium sorption of cesium by the buffer layer at 1800°C might provide an explanation for the narrow low-inventory peak in Fig. 1(*a*).

8.3 SPECULATION ON FURTHER ANALYSIS AND MODELLING

More than one failure/release mechanism must be considered for reproduction of the bimodal cesium inventory distribution. The Weibull distribution function is a standard approach to failure modelling of brittle materials and of MHTGR fuel performance. Inclusion of an additional diffusive release mechanism is one approach to reproducing the bimodal distribution. Another approach could consider the use of more than one Weibull distribution to characterize SiC failure, which results from more than one failure mechanism. This approach has been employed in fracture modelling of machined SiC specimens whose failure develops from both surface and edge flaws, with each characterized by a set of Weibull parameters. One can refer to Easler et al.[16] and Phani et al.[17] for additional information on this approach to modelling failure from multiple mechanisms.

The traditional approach of using a single diffusion coefficient or single effective diffusion coefficient is appropriate for diffusion in media that do not change in composition or structure over time. This situation is not representative of SiC during extended heating at high temperatures. A single diffusion coefficient could be used to realistically model neither decomposing SiC nor an ensemble of particles that have been subjected to a range of irradiation and temperature conditions, nor could it consider the random variation in microstructure arising from the manufacturing process. Reproduction of fission product release using a single diffusion coefficient must be considered more fortuitous than realistic.

The MGN model above used two discrete diffusion coefficients, with the failure function describing the temporal transition from one to the other. The distributions evident in Fig. 1(*a*) might also be reproduced by considering some particle-to-particle distribution of diffusion coefficients in SiC around the effective diffusion coefficient. It is not unreasonable

ORNL-DWG 93-12809

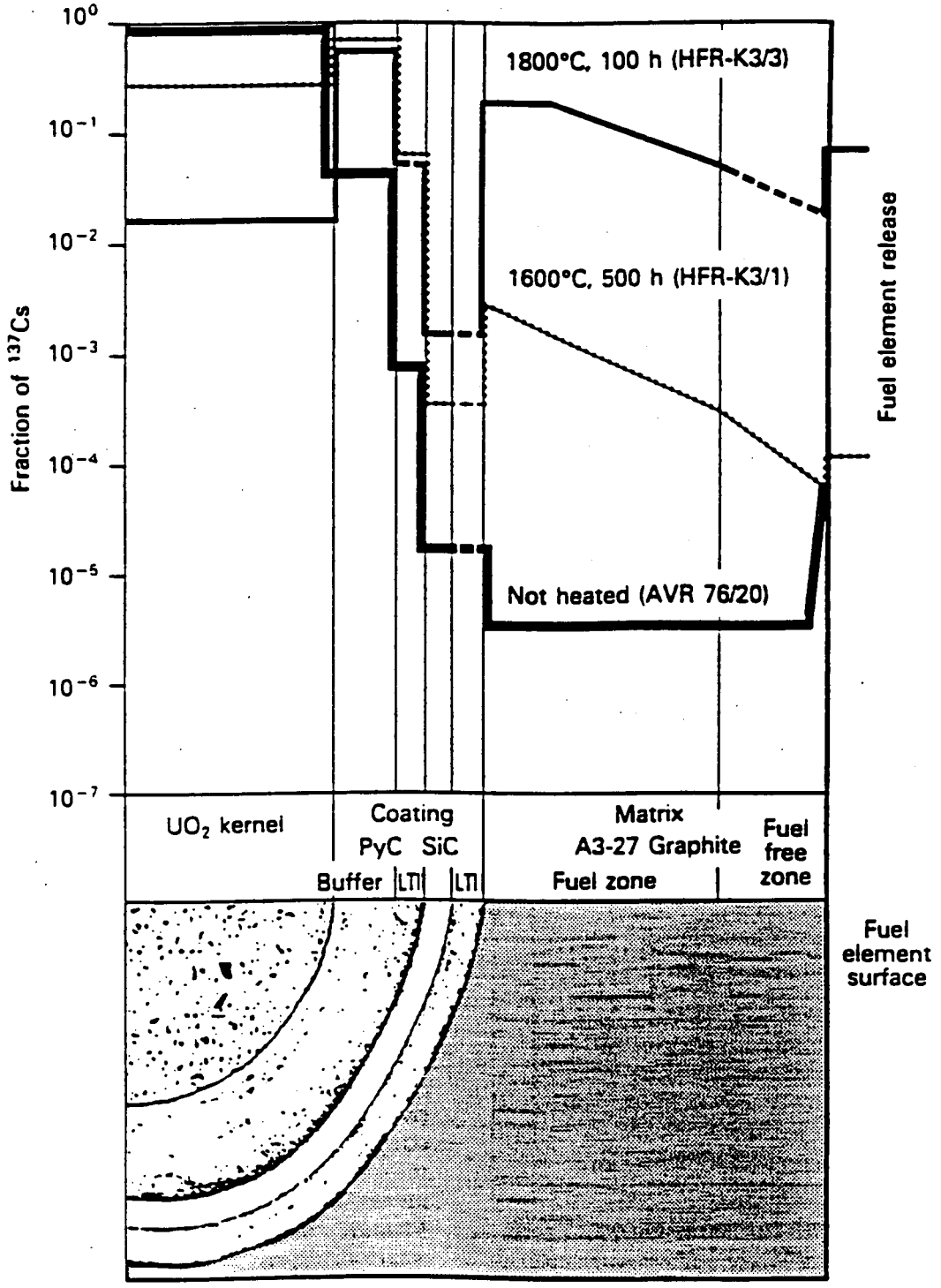

Fig. 8. Measured cesium-137 distributions in German particles and fuel spheres.[15]

to expect such a distribution to exhibit time dependence as the SiC evolves and ultimately decomposes at high temperatures. A less abrupt transition in diffusion coefficients than that assumed by the MGN model seems more likely except for cases of sudden SiC structural failure. Such considerations would broaden the calculated particle inventory distributions.

Röllig[18] applied the concept of a log-normal distribution of diffusion coefficients around the average to successfully approximate cesium-137 release from, and inventory in, German fuel sphere R2-K13/1 and in individual particles within the sphere.[6] This concept of variability in diffusion coefficients is a useful concept in further analysis of fission product release from individual particles.

The failure of IMGA to detect any particle with 100% cesium release after 100 h at 1800°C raises the question of whether a failed particle actually releases all its cesium. Although Bullock[19] reported 99% cesium release from several particles after heating at 1500°C for ~12,000 h, that time-at-temperature is not typical of reactor conditions and of the HFR-K3/3 heating test. In addition, Bullock's heating tests were periodically interrupted to permit gamma counting (i.e., repeated thermal cycling). Additional IMGA data on cesium inventories from failed particles heated to high temperatures would be helpful in evaluating the existing model for cesium release from failed particles and whether some equilibrium of cesium concentration or sorption within the particle coating layers, as suggested by Fig. 8, should be considered.

The concept of modelling cesium transport through failed SiC as a diffusion process, as employed in the MGN model, was suggested to provide some explanation for the range of particle-to-particle cesium inventories such as those evident in Fig. 1. The concept of surface diffusion of cesium through failed SiC is reasonable, but we have no data from which to approximate an effective surface diffusion coefficient. Fortunately, some piggyback samples in previous irradiation capsules were designed to obtain information on cesium transport through cracked SiC and may be able to provide insight and data for modelling this mechanism of cesium transport through and release from SiC.

9. CONCLUSIONS AND RECOMMENDATIONS

Cesium Release

1. No previously stated model for fission product release adequately explains the bimodal cesium-137 inventory distribution within the HFR-K3/3 particles.
2. The GN model does not reproduce the initial cesium-137 sphere release profile.
3. With appropriate values for model parameters, the MGN model can reproduce the intermediate cesium-137 inventory peak of the bimodal distribution. Incorporation of an additional failure mechanism represented by an enhanced diffusion coefficient can approximate the lower-inventory peak. This combined model qualitatively reproduces the bimodal distribution.
4. The width distribution of the SiC layer should not be disregarded when evaluating the distribution of cesium release from particles. The importance of this consideration is greater for the U.S. than the German particle design because of the larger variation in SiC thickness.
5. Failed particles retain some capacity for retention of cesium at 1800°C (i.e., nearly 20% of inventory).

Krypton Release

1. The assumptions of the GN model, as stated, do not reproduce the krypton-85 release curve.
2. The OPyC failure model may apply to the HFR-K3/3 data if approximately 1% OPyC failure is assumed.
3. If combined with the OPyC failure model, the GN model prediction is not inconsistent with the data.

Recommendations

1. Post-IMGA ceramographic inspection of the particles from both inventory peaks might be useful in verifying whether cracking of the SiC layer or other failure mechanisms is evident, and whether the failure mechanism is the same for the high- and intermediate-loss particles.
2. The MGN model should be used to evaluate additional German sphere release data to determine the applicability of the model and the consistency of the model parameters required to reproduce the data for the various spheres. Although the problems with mass balance between particle and sphere release make it doubtful that model parameters derived herein (based on IMGA data) can be applied directly to the release data for other spheres, the model methodology should be applied to evaluate the sphere-to-sphere consistency of the model.
3. The application of Röllig's[18] concept of a distribution of diffusion coefficients should be applied to the analysis of the HFR-K3/3 particle inventory data.
4. Several other German spheres have been reheated with some evidence of enhanced fission product release relative to singly heated spheres. The data from these spheres can be evaluated for consistency.
5. A modelling assumption of 1% OPyC failure appears promising in relating the German data for krypton release from the sphere to the concurrent cesium release and should be considered further.
6. If not previously evaluated, visual inspection of German particles after irradiation and after heating might provide information on whether irradiation-induced OPyC failure is evident as has been observed with U.S. particles.
7. A better treatment of the fraction of cesium retained by the matrix graphite is required prior to quantitative analysis of particle cesium release as derived from the overall sphere release. The approach taken by Goodin[5] in evaluating this matrix release fraction is too simplistic, and improvements such as a time-dependent matrix release fraction could be investigated, based on the work by Verfondern et al.[20]
8. The irradiation capsule piggyback samples, which were designed to study cesium transport along cracks in the SiC layer, should be evaluated to determine whether an effective diffusion coefficient could be derived to simulate this transport. If so, the value of this diffusion coefficient should be compared to the values used here to reproduce the IMGA data.

10. ACKNOWLEDGMENTS

I would like to express my appreciation to R. N. Morris, K. Sawa, and K. Verfondern for their review of this document and helpful comments. I also thank G. R. Carter for final report preparation, makeup, and quality assurance review, and K. Spence for editing.

11. REFERENCES

1. K. Verfondern, *Possible Explanation for HFR-K3/3 IMGA Results*, ORNL/M-2248, Martin Marietta Energy Systems, Inc., Oak Ridge Natl. Lab., September 1992.

2. C. A. Baldwin and M. J. Kania, "Fission Product Retention in TRISO Coated UO_2 Particle Fuels Subjected to HTR Simulated Core Heating Tests," in *Proceedings of the Specialists Meeting on Behaviour of Gas-Cooled Reactor Fuel Under Accident Conditions*, Oak Ridge, Tennessee, November 5-7, 1990, International Atomic Energy Agency, Vienna, Austria, 1990.

3. K. Verfondern, W. Schenk, and H. Nabielek, "Passive Safety Characteristics of Fuel for a Modular High-Temperature Reactor and Fuel Performance Modeling Under Accident Conditions," *Nucl. Technol.* 91, 235-46 (1990).

4. D. T. Goodin and H. Nabielek, *US/FRG Accident Condition Fuel Performance Models*, GA Technologies Report HTGR-85 107, Rev. 1, General Atomics, San Diego, 1985.

5. D. T. Goodin, *US/FRG Accident Condition Fuel Performance Models*, General Atomics Report DOE-HTGR-85107, Rev. A, General Atomics, San Diego, 1989.

6. W. Schenk and H. Nabielek, *Kugelbrennelemente mit TRISO-Partikeln bei Störfalltemperaturen (Zahlenwerk zum Bericht Jül-2091 und neue Ergebnisse von 1986 bis Oktober 1988)*, Kernforschungsanlage Jülich GmbH Report Jül-Spez-487, KFA Jülich, Germany, 1989.

7. R. C. Martin, "Diffusion Modeling of Fission Product Release During Depressurized Core Conduction Cooldown Conditions," in *Proceedings of the Specialists Meeting on Behaviour of Gas-Cooled Reactor Fuel Under Accident Conditions*, Oak Ridge, Tennessee, November 5-7, 1990, International Atomic Energy Agency, Vienna, Austria, 1990.

8. J. L. Martin and H. Nabielek, *Modelling of Fuel Element Heating Tests*, Kernforschungsanlage Jülich GmbH Technical Note HBK-TN-4/88, KFA Jülich, Germany, 1988.

9. B. F. Myers, *Cesium Diffusion in Silicon Carbide During Post Irradiation Anneals*, Kernforschungsanlage Jülich GmbH Technical Note HBK-TN-01/84, KFA Jülich, Germany, 1984.

10. W. Schenk, D. Pitzer, and H. Nabielek, *Fission Product Release Profiles from Spherical HTR Fuel Elements at Accident Temperatures*, Kernforschungsanlage Jülich GmbH Report Jül-2234, KFA Jülich, Germany, 1988.

11. General Atomics, *Fuel Product Specification for Irradiation Capsule HRB-21*, U.S. DOE Report DOE-HTGR-88539, General Atomics, San Diego, 1991.

12. W. J. Kovacs, K. Bongartz, and D. T. Goodin, "High-Temperature Gas-Cooled Reactor Fuel Pressure Vessel Performance Models," *Nucl. Technol.* **68**, 344-54 (1985).

13. K. Verfondern, T. D. Dunn, and J. M. Bolin, *Comparison of US/FRG Accident Condition Models for HTGR Fuel Failure and Radionuclide Release*, Forschungszentrum Jülich GmbH Report Jül-2458, KFA Jülich, Germany, March 1991.

14. J. W. Ketterer and B. F. Myers, *Capsule HRB-16 Postirradiation Examination Report*, U.S. DOE Report HTGR-85-053, General Atomics, San Diego, 1985.

15. W. Schenk and H. Nabielek, "High-Temperature Reactor Fuel Fission Product Release and Distribution at 1600 to 1800°C," *Nucl. Technol.* **96**, 323-36 (1991).

16. T. E. Easler, R. C. Bradt, and R. E. Tressler, "Concurrent Flaw Populations in SiC," *J. Am. Ceram. Soc.* **64**(3), C-53–C-55 (1981).

17. K. K. Phani and A. K. De, "Evaluation of Concurrent Flaw Populations in Silicon Carbide in Terms of a Modified Weibull Distribution Function," *J. Am. Ceram. Soc.* **71**(4), C-196–C-197 (1988).

18. K. Röllig, "Capabilities of the Diffusion Model for Metallic Fission Products at Temperature Transients up to 1600°C - Case: Cs-137 Release from Spherical Fuel Element R2-K13/1," Technical Workshop on Unification of Coated Particle Performance Models and Fission Product Transport Data for the HTR, Forschungszentrum Jülich, Germany, December 2-4, 1991, International Atomic Energy Agency, Vienna, Austria, 1991.

19. R. E. Bullock, *Fission-Product Release During Postirradiation Annealing of Several Types of Coated Fuel Particles*, GA Technologies Report GA-A17046, General Atomics, San Diego, 1983.

20. K. Verfondern and D. Müller, *Code Development for Fission Product Behavior in HTR Fuel for Safety Assessments*, Kernforschungsanlage Jülich GmbH Report KFA–ISF–IB-10/89, KFA Jülich, Germany, 1989.

APPENDIX A: SHELL CODE DEVELOPMENT

The SHELL code as described by R. C. Martin* incorporates a simple analytical model for diffusion through and release from a single thin shell. This code is useful for scoping studies in model development in those situations where diffusion through one concentric coating layer is rate determining (in our case, either through intact SiC layers for cesium diffusion or through failed SiC/intact OPyC layers for krypton diffusion). SHELL is based on the following analytical equation:

$$FR = \frac{3\,b\,(b-a)}{a^2}\left\{\frac{D\,t}{(b-a)^2} - \frac{1}{6} - \frac{2}{\pi^2}\sum_{n=1}^{\infty}\frac{(-1)^n}{n^2}\exp\left[\frac{-n^2\pi^2 D\,t}{(b-a)^2}\right]\right\} , \qquad \text{(A1)}$$

with FR the fractional release, a and b the radii of the inner and outer surfaces of the shell, respectively, D the diffusion coefficient, and t the time.

This formulation assumes a constant internal fission product concentration, which is acceptable for small values of FR, but overstates the release as FR approaches one. As formulated, the fractional release can exceed one, a result which is nonphysical.

An alternative analytical formulation commonly employed for scoping studies is attributed to H. Nabielek and referenced by J. L. Martin et al.:†

$$FR = 1 - \left(1 + \frac{\gamma}{2}\right) e^{-3\gamma D^* t} , \qquad \text{(A2)}$$

$$D^* = \frac{D}{d^2} , \qquad \text{(A3)}$$

$$\gamma = \frac{d}{r} , \qquad \text{(A4)}$$

where

D = diffusion coefficient of the fission product in the coating layer ($m^2\ s^{-1}$),
d = thickness of the coating layer (m),
r = inner radius of the coating layer (m),
t = time (s).

---

*R. C. Martin, "Diffusion Modeling of Fission Product Release During Depressurized Core Conduction Cooldown Conditions," in *Proceedings of the Specialists Meeting on Behaviour of Gas-Cooled Reactor Fuel Under Accident Conditions*, Oak Ridge, Tennessee, November 5-7, 1990, International Atomic Energy Agency, Vienna, Austria, 1990.

†J. L. Martin and H. Nabielek, *Modelling of Fuel Element Heating Tests*, Kernforschungsanlage Jülich GmbH Technical Note HBK-TN-4/88, KFA Jülich, Germany, 1988.

For an assumed diffusion coefficient of 10^{-14} m^2 s^{-1}, the fractional release through a 40-μm shell of 420–μm internal radius (corresponding to the OPyC layer of the particles in sphere HFR-K3/3) as calculated by the two methods is shown in Fig. A.1. Agreement between the two methods is good for releases up to 10% and more, but SHELL greatly overstates the release after extended heating times. A more complex analytical formulation such as that developed by Morgan et al.* would correct this error. However, to save time, the use of a reduction factor was explored that would provide agreement between the predictions of SHELL and the Nabielek equation at larger fractional releases. It was found that the fractional release, *FR*, calculated from Eq. (A1) could be used in the transformation:

$$FR' = \frac{FR}{1 + \frac{FR}{1.4}} , \qquad \text{(A5)}$$

ORNL-DWG 93-12810

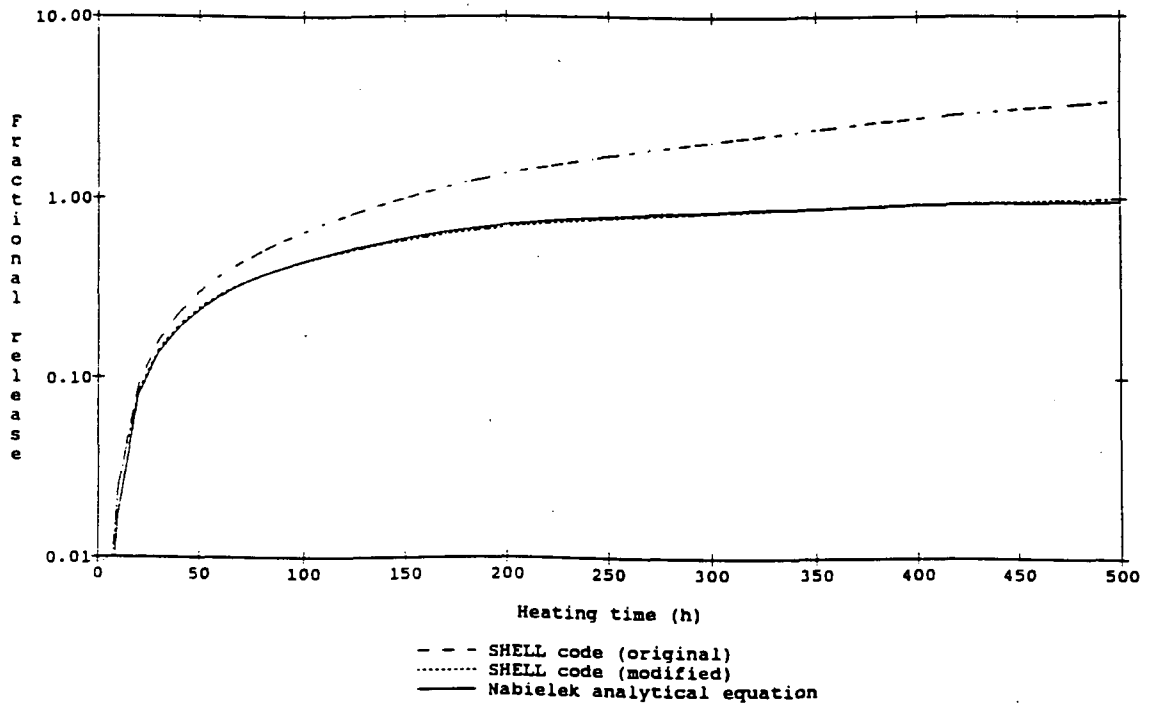

Fig. A.1. Comparison of fractional release predictions through OPyC layer using the analytical equation of H. Nabielek, using SHELL code, and using modified SHELL code. Diffusion coefficient of 10^{-14} m^2 s^{-1} was assumed.

---

*M. T. Morgan and A. P. Malinauskas, "Cesium Release Transport in Biso-Coated Fuel Particles," *Nucl. Technol.* 35, 457-64 (1977).

which provided the modified fractional release, *FR'*, presented in Fig. A.1 that was in much better agreement with the Nabielek analytical equation. In the future, the formulation of Morgan et al.* could be implemented into SHELL for self-consistent quantitative reliability of the results, rather than just applying a correction factor based on the predictions of Nabielek's equation.

Figure A.2(*a*) gives results analogous to Fig. A.1 using the reference diffusion coefficient of Eq. (A4) for krypton in PyC at 1800°C. Figure A.2(*b*) reproduces Fig. A.2(*a*) using a linear scale, indicating that SHELL predictions are more accurate at very low values of fractional release than are those of the Nabielek equation.

---

*M. T. Morgan and A. P. Malinauskas, "Cesium Release Transport in Biso-Coated Fuel Particles," *Nucl. Technol.* 35, 457-64 (1977).

ORNL-DWG 93-12811

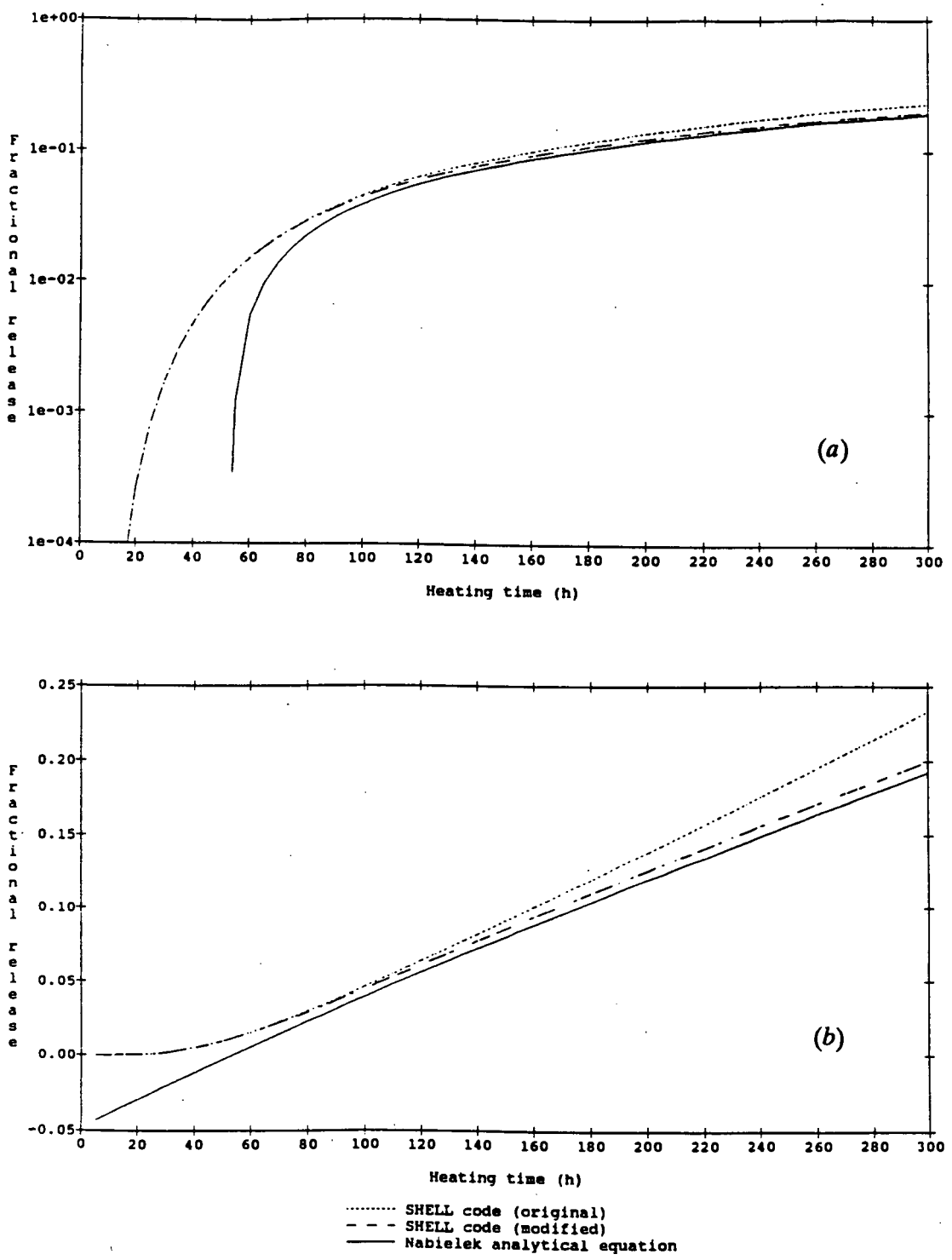

Fig. A.2. Comparison of fractional release predictions of krypton-85 through OPyC layer at 1800°C using the analytical equation of H. Nabielek, using SHELL code, and using modified SHELL code: (*a*) log scale and (*b*) linear scale.

INTERNAL DISTRIBUTION

1-2. Central Research Library
3. Document Reference Section
4-5. Laboratory Records Department
6. Laboratory Records, ORNL-RC
7. ORNL Patent Section
8-10. M&C Records Office
11. C. A. Baldwin
12. W. P. Barthold
13. J. C. Cleveland
14. D. F. Craig
15. F. J. Homan
16. H. Jones
17. M. J. Kania
18. O. F. Kimball
19-23. R. C. Martin
24. R. N. Morris
25. B. F. Myers
26. N. H. Packan
27. P. L. Rittenhouse
28. O. M. Stansfield
29. A. W. Trivelpiece
30. R. P. Wichner

EXTERNAL DISTRIBUTION

31-36. CEGA, P.O. Box 85608, San Diego, CA 92186-9784

R. M. Forssell
D. L. Hanson
D. W. McEachern
A. J. Neylan
W. J. Scheffel
C. A. Young

37-39. EG&G IDAHO, INC., NPR DOCUMENT CENTRAL CENTER (DCC) P.O. Box 1625, Attn.: MS 2520, Idaho Falls, ID 83415-2520

R. K. McCardell
M. L. Russell
F. H. Southworth

40-41. GENERAL ATOMICS, INC., P.O. Box 85608, San Diego, CA 92186-9784

G. C. Bramblett
R. F. Turner

42-43. MODULAR HTGR PLANT DESIGN CONTROL OFFICE, P.O. Box 85608, San Diego, CA 92138

J. Kendall
R. R. Mills

44. DOE, OFFICE OF ADVANCED REACTOR PROGRAMS, Washington, DC 20585

    Director

45. DOE, OFFICE OF ADVANCED REACTOR PROGRAMS, Division of HTGRs, NE-451, Washington, DC 20585

    P. M. Williams

46. DOE, SAN FRANCISCO OPERATIONS OFFICE, 1333 Broadway, Oakland, CA 94612

    S. El-Safwany

47. DOE, OAK RIDGE OPERATIONS OFFICE, P.O. Box 2001, Oak Ridge, TN 37831-6269

    Office of Assistant Manager for Energy Research and Development

48-49. DOE, OFFICE OF SCIENTIFIC AND TECHNICAL INFORMATION, P.O. Box 62, Oak Ridge, TN 37831

    For distribution by microfiche as shown in DOE/OSTI-4500, Distribution Category UC-522T (Gas-Cooled Reactor Technology)